Identification of new gene inhibiting Gemcitabine resistance in pancreatic cancer

Kim Minsoo

Department of Medical Science

Graduate School

Yonsei University

Identification of new gene inhibiting Gemcitabine resistance in pancreatic cancer

Advisor Jae-Ho Cheong

A Master's Thesis Submitted
to the Department of Medical Science
and the Committee on Graduate School
of Yonsei University in Partial Fulfillment of the
Requirements for the Degree of
Master of Medical Science

Kim Minsoo

June 2025

Identification of new gene inhibiting Gemcitabine resistance in pancreatic cancer

This Certifies that the Master's Thesis of Minsoo Kim is Approved

Committee Chair	Sungsoon Fang
Committee Member	Joon Seong Park
Committee Member	Jae-Ho Cheong

Department of Medical Science
Graduate School
Yonsei University
June 2025

ACKNOWLEDGEMENTS

I sincerely thank my academic advisors, Professor Joon Seong Park and Professor Hyo Jung Kim, for their invaluable support and insightful guidance throughout the course of my graduate studies.

I am sincerely thankful to my laboratory colleagues, Woosol Chris Hong, Juhyun Kim, and Hyeon Woong Kang, for their continuous support and collaboration during my research. Their contributions and thoughtful discussions greatly enriched my academic experience.

I also wish to extend my appreciation to Wongeon Yoon and Dongyong Lee for their efforts in providing and analyzing the clinical data, which served as a critical component of this study. Special thanks to Taebok Lee for his assistance in conducting mitochondria-related experiments.

Lastly, I am profoundly grateful to my parents for their unconditional love, patience, and encouragement, which have supported me throughout this academic journey.

TABLE OF CONTENTS

LIST OF FIGURES

ABSTRACT

Identification of new gene inhibiting Gemcitabine resistance in pancreatic cancer

Pancreatic cancer is a aggressive disease with dismal clinical outcomes, primarily owing to its swift acquisition of resistance to chemotherapeutic agents. Among the diverse factors influencing therapy failure, mitochondrial dynamics have emerged as key contributors to cancer cell survival. Despite its clinical relevance, the molecular basis underlying gemcitabine resistance in pancreatic cancer has not been fully elucidated. This study highlights the myo-inositol:sodium symporter SLC5A3 (solute carrier family 5 member 3) as a contributor to gemcitabine resistance in pancreatic cancer. SLC5A3 was markedly upregulated in gemcitabine-resistant pancreatic cancer tissues and cell lines, where it supported cell survival by maintaining mitochondrial stability and suppressing apoptotic pathways. Functional experiments revealed that silencing SLC5A3 led to altered mitochondrial dynamics, elevated ROS levels, increased mitochondrial fragmentation, and a reduction in oxidative phosphorylation efficiency. Additionally, SLC5A3 depletion activated PINK1/Parkin-mediated mitophagy, leading to excessive clearance of both damaged and functional mitochondria. This mitochondrial depletion resulted in an energy crisis and heightened apoptotic susceptibility. In animal models, the inhibition of SLC5A3 markedly strengthened gemcitabine's antitumor activity, leading to suppressed tumor progression in xenograft experiments. These results underscore the importance of SLC5A3 in maintaining mitochondrial stability and propose it as a promising candidate for therapeutic intervention against chemoresistance in pancreatic cancer.

Key words: pancreatic cancer, gemcitabine, resistance, mitochondrial dysfunction, mitophagy

1. INTRODUCTION

As the leading and most lethal form of pancreatic cancer, pancreatic ductal adenocarcinoma (PDAC) is associated with a 5-year survival rate near 13%, reflecting its severe clinical outcome. [1] Due to limited therapeutic strategies and the rapid progression of the disease, gemcitabine remains the cornerstone chemotherapeutic agent for PDAC treatment. [2] However, its clinical effectiveness is often undermined by the rapid emergence of drug resistance. Several mechanisms have been implicated in gemcitabine resistance, including activation of survival-promoting pathways, alterations in drug metabolism, and suppression of apoptotic responses. [3,4,5,6] Despite these insights, the intricate regulatory mechanisms and core molecular contributors underlying gemcitabine resistance in PDAC are not fully understood. Therefore, identifying novel targets and understanding the cellular basis of chemoresistance are essential to improving therapeutic outcomes.

Mitochondria play a critical role in both energy metabolism and apoptotic signaling, and increasing evidence implicates mitochondrial dysfunction in cancer drug resistance. [7,8,9] Tumor cells rely on a finely tuned interplay between mitochondrial fission and fusion to adapt to metabolic stress and sustain survival. [10] Disruption of mitochondrial dynamics increases susceptibility to oxidative damage, subsequently triggering mitophagy. [11,12] Although mitophagy serves to eliminate dysfunctional mitochondria and maintain cellular health, its excessive activation can lead to depletion of functional mitochondria, resulting in reduced ATP generation and increased susceptibility to apoptosis. [13,14,15,16] Thus, understanding how mitophagy is regulated in chemoresistant cancer cells may uncover potential therapeutic vulnerabilities.

As the largest class of membrane transporters, SLC proteins are increasingly linked to key processes in metabolism and cancer progression. [17,18,19] Among them, SLC5A3 has emerged as a critical player in cancer biology. SLC5A3 facilitates cellular osmoregulation and inositol uptake, contributing to cell proliferation and survival in various malignancies. [20,21] Previous studies have demonstrated its oncogenic roles in acute myeloid leukemia, lung cancer, and cervical cancer by modulating metabolic signaling and gene expression pathways. [22,23,24]

Our analysis revealed that SLC5A3 levels were substantially higher in PDAC samples and cells exhibiting resistance to gemcitabine. Functional analyses indicated that silencing SLC5A3 disrupted mitochondrial performance, led to diminished oxidative phosphorylation (OXPHOS), elevated intracellular reactive oxygen species (ROS) levels, and triggered apoptotic cell death. Furthermore, SLC5A3 knockdown disrupted mitochondrial dynamics and triggered mitophagy, which in turn led to the degradation of both damaged and intact mitochondria, exacerbating energy depletion and apoptotic sensitivity. These findings suggest that targeting SLC5A3 could enhance therapeutic efficacy by reversing chemoresistance through the modulation of mitophagy and mitochondrial homeostasis.

2. MATERIALS AND METHODS

2.1. Ethical compliance and human sample collection

All procedures involving human-derived tissues were conducted under ethical oversight, in accordance with the principles outlined in the Declaration of Helsinki. Research protocols received approval from the Institutional Review Boards of Gangnam Severance Hospital (approval number: 3-2021-0414) and Seoul National University Hospital (approval number: H-1705-031-852). Pancreatic tissues were sourced from patients with histologically confirmed PDAC or from individuals without malignancy, all undergoing surgical procedures at Gangnam Severance Hospital. Patients who received standard gemcitabine therapy (1,000 mg/m² weekly for several cycles) were stratified based on recurrence within six months. Informed consent was obtained from each participant.

2.2. Data sources and computational methods

Public datasets, including TCGA–PAAD and Seoul National University Hospital cohorts, were analyzed for survival correlation. Expression levels of SLC5A3 were divided into two groups using statistical thresholds identified via X-tile (version 3.6.1; Yale University, Chicago, IL, USA). Survival analyses were visualized using GraphPad Prism software (v10.3.0; GraphPad, San Diego, CA, USA).

2.3. Cell lines and induction of drug resistance

Commercially available PDAC cell lines were acquired from ATCC (Gaithersburg, MD, USA). They were sustained in either RPMI-1640 or DMEM media supplemented with 10% serum and antibiotics (Biowest, Lyon, France; Gibco, Toronto, Canada). To establish resistance, PANC-1 cells were incrementally treated with sub-cytotoxic concentrations of gemcitabine (Yuhan, Daejeon, Republic of Korea) over several weeks, ultimately stabilizing at 0.5 μM.

2.4. Proliferation and cycle analysis

Cell viability was assessed by a tetrazolium-based metabolic assay (EZ-Cytox; DoGenBio, Busan, Korea). Approximately 5,000 cells were plated per well and treated with gemcitabine for 72 hours, followed by reagent incubation. Optical density was measured at 450 nm using a microplate reader (Molecular Devices, Birmingham, UK). For DNA synthesis assessment, BrdU incorporation was measured via immunofluorescence. Cell cycle distribution was quantified using propidium iodide and RNase A staining, analyzed on a flow cytometer (BD Biosciences, Vienna, Austria).

2.5. Detection of apoptotic and oxidative responses

Apoptosis was evaluated by Annexin V staining (BD Biosciences, Vienna, Austria) and DNA

fragmentation using a TUNEL kit (Abcam, Madrid, Spain). Reactive oxygen species levels were measured through DCFDA staining (Sigma-Aldrich, Milan, Italy), and signals were recorded using a flow cytometry-based system. Data processing was conducted with FlowJo (version 10.8.1; FlowJo LLC, Dublin, Ireland).

2.6. Mitochondrial performance and bioenergetics

Functional analyses of mitochondrial respiration were carried out using Seahorse instruments (Agilent Technologies, Amsterdam, Netherlands). Oxygen consumption and ATP output were measured following manufacturer instructions using assay kits compatible with the XFp and XFe96 platforms. Organelle fractionation was performed using a mitochondria isolation protocol (Thermo Fisher Scientific, Munich, Germany).

2.7. Microscopy-based phenotypic profiling

Cells were stained with mitochondrial and nuclear dyes and imaged using an automated confocal system (Operetta CLS; PerkinElmer, Sydney, Australia). Image classification was processed using built-in machine learning software. For ultrastructural observation, fixed samples underwent transmission electron microscopy (JEM-1400 Flash; JEOL, Osaka, Japan).

2.8. Mouse xenograft experiments

BALB/c (Orient Bio, Incheon, Republic of Korea) were surgically implanted with PDAC cells mixed with extracellular matrix gel. Short-hairpin RNA vectors targeting SLC5A3 (Origene, Paris, France) were administered intravenously. Gemcitabine and CCCP were injected intraperitoneally. Animal studies were approved by Yonsei University IACUC (approval no. 2022-0061).

2.9. Immunostaining and imaging

Tissue sections (5 μm) were processed for immunofluorescence microscopy. Following antigen retrieval and blocking, samples were incubated with primary antibodies and then fluorophore-conjugated secondaries (Invitrogen, Singapore; Jackson ImmunoResearch, Berlin, Germany). Imaging was performed using a laser-scanning confocal system (Leica TCS SP8 STED CW; Leica Microsystems, Zurich, Switzerland).

2.10. Analysis of gene expression

Total RNA was extracted using phenol–chloroform reagents (TRIzol; Invitrogen, Singapore) and reverse transcribed. Real-time amplification was performed using SYBR Green chemistry (Applied Biosystems, Tel Aviv, Israel). For transcriptome profiling, libraries were constructed using QuantSeq kits (Lexogen, Seoul, Republic of Korea) and sequenced on a NextSeq 550 (Illumina, Jakarta, Indonesia). Pathway analyses were conducted using DAVID and R (v3.5.1).

2.11. Immunoblot protocol

Protein extracts were isolated in lysis buffer containing both protease and phosphatase inhibitor cocktails (Rockland, Nice, France). Equal volume of lysate were segregated by Sodium Dodecyl Sulfate - Polyacrylamide Gel Electrophoresis, moved to Polyvinylidene Difluoride membranes (Merck Millipore, Zurich, Switzerland), and probed with specific antibodies. Visualization was achieved using chemiluminescence reagents and documented with imaging systems (GE Healthcare, Melbourne, Australia).

2.12. Gene silencing by RNA interference

Transient knockdown of SLC5A3 was achieved through transfection of siRNA oligonucleotides (Santa Cruz Biotechnology, New Delhi, India) using lipid-based reagents (Lipofectamine RNAiMAX; Invitrogen, Singapore). Analyses were performed 48–72 hours post-transfection.

2.13. Statistical evaluation

All data were obtained from at least three independent experiments unless otherwise indicated. Results are presented as means ± standard deviation (SD). Statistical significance was determined using one-way or two-way ANOVA, with p-values < 0.05 considered significant. All analyses were performed using GraphPad Prism software (version 10.3; GraphPad Software, San Diego, CA, USA).

3. RESULTS

3.1. SLC5A3 expression is increased in PDAC

RNA-seq analysis of PDAC tumors and adjacent non-tumor tissues was carried out to explore the role of solute carrier (SLC) transporters in disease development. SLC5A3 was identified as the most prominently upregulated member of the SLC gene family in pancreatic tumor tissues relative to their matched adjacent normal counterparts (Figure 1A). This observation was further substantiated by experimental validation showing consistent upregulation of SLC5A3 at both transcript and protein levels in PDAC samples (Figure 1B), implying its potential involvement in pancreatic tumor biology.

To determine whether elevated SLC5A3 expression is unique to PDAC or observed across different tumor types, we examined data from GEPIA2 database. SLC5A3 was found to be overexpressed in multiple malignancies, with pancreatic adenocarcinoma (PAAD) displaying the highest relative expression (Figure 1C). [27,28] Data integration from TCGA and GTEx cohorts validated the observation of increased SLC5A3 expression in PAAD, showing a significant elevation relative to non-tumorous pancreatic tissue. (Figure 1D). [29,30,31]

We next assessed SLC5A3 expression across different tumor stages, and the data revealed persistently high expression levels as the disease progressed, suggesting that SLC5A3 may contribute to disease advancement. Survival analysis using cohorts from TCGA–PAAD and Seoul National University (SNU) revealed a statistically significant association between high SLC5A3 expression and reduced overall survival, suggesting a potential prognostic role in PDAC (Figure 1E).

To understand the transcriptional impact of SLC5A3 in PDAC, we conducted a clustered heatmap analysis using RNA-seq data. Patients with high versus low SLC5A3 expression observed distinct gene expression patterns, indicating that SLC5A3 may regulate specific gene networks in the tumor microenvironment (Figure 1F). Moreover, differential gene expression analysis using the GSE62452 dataset identified SLC5A3 among the top upregulated genes in PDAC tumor samples when compared to normal controls (Figure 1G). Further investigation through Gene Ontology (GO) enrichment analysis revealed that genes strongly correlated with SLC5A3 were enriched in pathways related to mitochondrial function, apoptotic signaling, and regulation of the cell cycle (Figure 1H). [32]

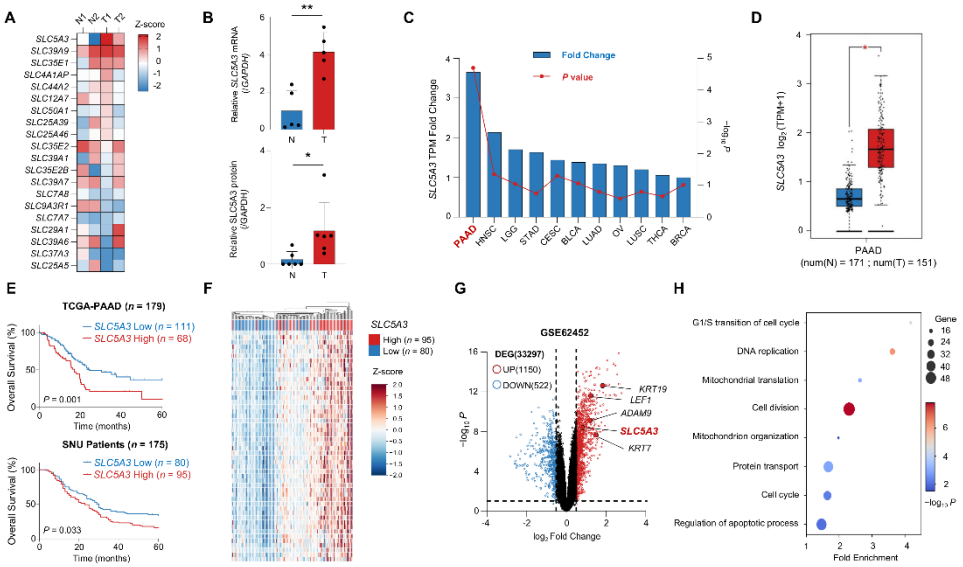

Figure 1. SLC5A3 expression is increased in PDAC. (A) Using RNA sequencing data from Gangnam Severance Hospital, we visualized differences in SLC gene expression between pancreatic tumors and adjacent non-tumorous tissues through a heatmap analysis. (B) Analysis of paired tumor and normal tissues demonstrated a marked increase in SLC5A3 expression at both the transcript and protein levels in PDAC. (C) Among multiple cancer types analyzed using GEPIA2 and Human Protein Atlas, SLC5A3 was most prominently expressed in pancreatic adenocarcinoma. (D) Boxplot comparisons using TCGA and GTEx datasets indicate significantly higher SLC5A3 transcript levels in PDAC tissues. (E) Survival analyses using Kaplan–Meier curves from both TCGA–PAAD and SNU datasets. (F) Hierarchical clustering of SNU cohort transcriptomic data illustrates distinct gene expression profiles based on SLC5A3 expression levels. (G) Volcano plot from GSE62452 dataset highlights SLC5A3 as one of the most significantly upregulated genes in PDAC. (H) GO analysis of SLC5A3-correlated genes indicates enrichment in pathways related to mitochondrial activity, apoptosis regulation, and cell cycle control.

3.2. Elevated SLC5A3 is associated with chemoresistance and poor prognosis

To further explore the involvement of SLC5A3 in therapeutic response, we evaluated its expression and correlation with gemcitabine resistance in both clinical samples and cell models of pancreatic ductal adenocarcinoma (PDAC). Patients classified as gemcitabine-resistant exhibited markedly elevated SLC5A3 levels compared to their gemcitabine-sensitive counterparts (Figure 2B). This supports the hypothesis that SLC5A3 contributes to acquired chemoresistance.

We also examined SLC5A3 expression in a panel of pancreatic cancer cell lines previously characterized for their sensitivity to gemcitabine. Across these cell lines, RES variants consistently showed upregulation of SLC5A3 compared to their SEN counterparts, reinforcing its conserved association with resistance (Figure 2E). Consistently, protein and mRNA levels of SLC5A3 were markedly elevated in RES PDAC tumor tissues relative to SEN tissues (Figure 2D). To functionally validate this correlation, we performed WST-1 viability assays to determine the gemcitabine IC50 values in SEN and RES PANC-1 cells. The results demonstrated that RES cells required substantially higher concentrations of gemcitabine to achieve comparable cytotoxicity, indicating increased drug tolerance (Figure 2F).

We then turned our attention to known molecular mediators of gemcitabine resistance. Among these, RRM1 emerged as the gene most strongly correlated with SLC5A3 expression in the TCGA–PAAD cohort (Figure 2C). [33] Subsequent co-expression analyses confirmed that both RRM1 and SLC5A3 were elevated in resistant cells and tissues, suggesting that they may function in a coordinated manner to promote resistance.

In clinical datasets, survival outcomes were evaluated to determine the prognostic relevance of SLC5A3. Patients within the SNU cohort exhibiting high SLC5A3 expression had significantly shorter relapse-free survival compared to those with lower expression levels, implying that SLC5A3 may serve as a predictive indicator for poor response to gemcitabine (Figure 2A).

Lastly, to identify common molecular features of resistance, transcriptomic data from RES PANC-1 cells, RES patient tissues, and PDAC tumor tissues were compared. Analysis of the Venn diagram identified nine commonly upregulated genes, including SLC5A3, across all datasets examined (Figure 2G), suggesting a core set of molecular features associated with chemoresistant phenotypes.

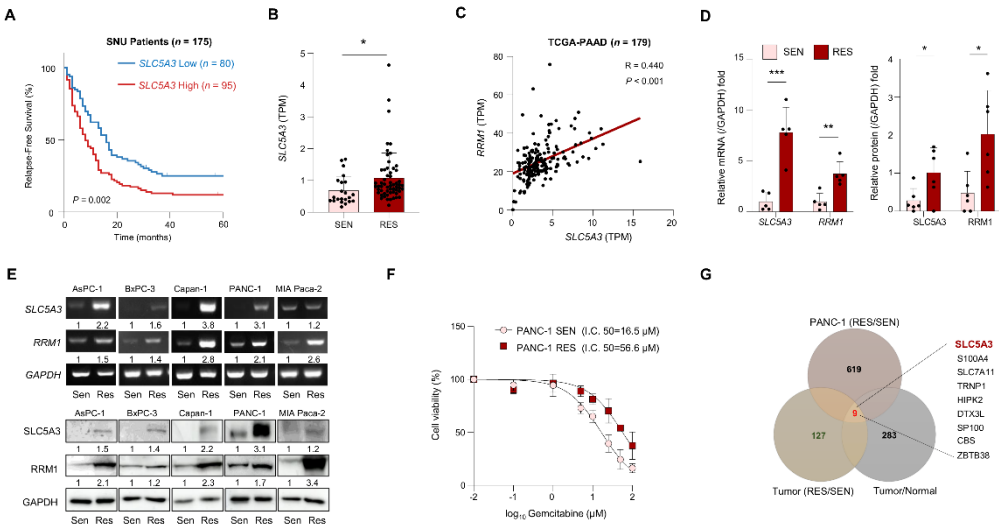

Figure 2. Elevated SLC5A3 is associated with chemoresistance and poor prognosis. (A) High SLC5A3 expression correlated with shorter relapse-free survival in the SNU cohort, indicating an association with earlier tumor recurrence. (B) Patients classified as gemcitabine-resistant (RES) exhibited markedly elevated SLC5A3 expression levels relative to those in the gemcitabine-sensitive (SEN) group. (C) Scatter plot analysis shows a strong correlation between SLC5A3 and the chemoresistance marker RRM1 in TCGA–PAAD samples. (D) Both SLC5A3 and RRM1 exhibited elevated mRNA and protein expression in RES tumor tissues, supporting their coordinated upregulation in gemcitabine resistance. (E) SLC5A3 and RRM1 were also highly expressed in multiple gemcitabine-resistant PDAC cell lines. (F) Dose–response curve and IC50 analysis of PANC-1 cells revealed increased resistance in RES cells. (G) A Venn diagram comparing upregulated genes from RES PANC-1 cells, RES patient tissues, and GSE62452 tumor samples identified SLC5A3 among the commonly upregulated genes.

3.3. SLC5A3 depletion limits proliferation in GR PDAC

We performed targeted gene silencing in pancreatic ductal adenocarcinoma (PDAC) cells that had acquired resistance to gemcitabine. Specific siRNAs were used to downregulate SLC5A3 expression in resistant (RES) cells, while scrambled siRNA served as a negative control. Subsequent validation confirmed effective knockdown of SLC5A3 at both the transcriptional and protein levels (Figure 3A, B).

Since SLC5A3 is involved in myo-inositol uptake, we assessed intracellular levels of this metabolite following knockdown. A significant decline in myo-inositol content was observed in SLC5A3-silenced cells (Figure 3C). [34,35] This metabolic disturbance was paralleled by a marked decrease in cell viability, as determined by WST assays. Although RES cells displayed increased viability compared to their sensitive (SEN) counterparts, this effect was notably reversed upon suppression of SLC5A3 (Figure 3D).

In addition, mRNA expressions of both SLC5A3 and RRM1 were reduced in knockdown cells, suggesting that impaired inositol transport might be linked to broader effects on survival-related gene networks. To explore these pathways, we employed gene set enrichment analysis (GSEA), which revealed that RES cells were enriched in gene sets related to mitotic processes, including chromosome segregation and checkpoint control. These gene sets were significantly diminished in SLC5A3 knockdown cells (Figure 3E). [36]

Cell cycle analysis using flow cytometry demonstrated that silencing SLC5A3 led to accumulation of cells in the G0/G1 phase, alongside a reduction in S phase populations, consistent with a G1 phase arrest (Figure 3F). To probe the molecular mechanisms underlying this shift, we quantified expression levels of critical regulators of cell cycle progression. Cyclins and CDKs including CCND1, CCNE, CDK4, and CDK6 were substantially elevated in RES cells but significantly decreased upon SLC5A3 knockdown (Figure 3G, H). To further assess proliferation, Ki-67 immunofluorescence staining was used. A larger proportion of RES cells stained positive for Ki-67 relative to SEN cells. However, SLC5A3 depletion led to a pronounced decline in proliferative cell numbers (Figure 3I, J). In addition to proliferation, we investigated migratory potential via wound healing assays. As expected, RES cells exhibited enhanced migratory capacity, whereas SLC5A3 knockdown impaired wound closure and cell movement (Figure 3K).

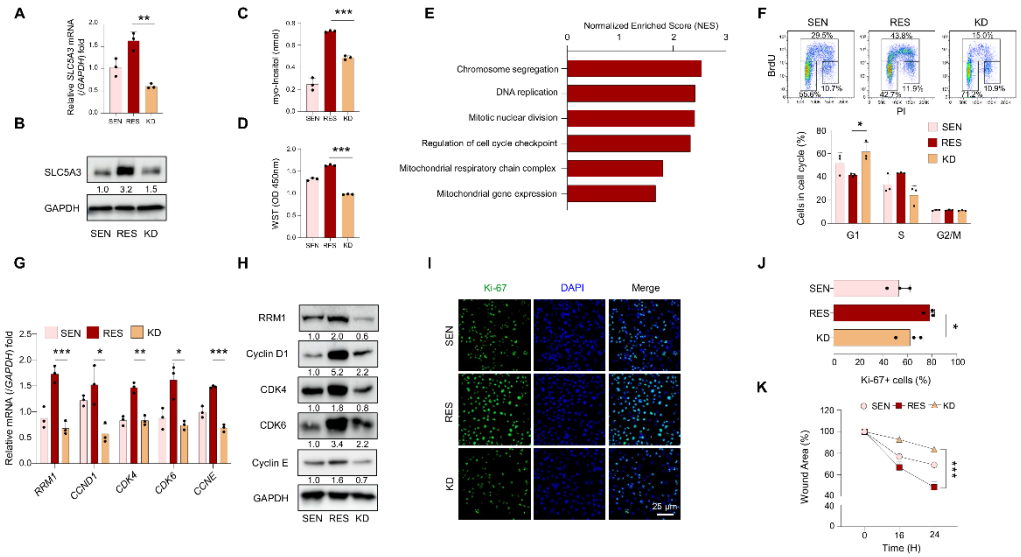

Figure 3. SLC5A3 depletion limits proliferation in GR PDAC. (A) High SLC5A3 expression was associated with earlier tumor recurrence, as shown by relapse-free survival data from the SNU cohort. (B) Patients classified as gemcitabine-resistant (RES) exhibited markedly elevated SLC5A3 expression levels relative to those in the gemcitabine-sensitive (SEN) group. (C) Scatter plot analysis shows a strong correlation between SLC5A3 and the chemoresistance marker RRM1 in TCGA–PAAD samples. (D) Both SLC5A3 and RRM1 exhibited elevated mRNA and protein expression levels in RES tumor tissues, supporting their coordinated upregulation in gemcitabine resistance. (E) SLC5A3 and RRM1 were also highly expressed in multiple gemcitabine-resistant PDAC cell lines. (F) Dose–response curve and IC50 analysis of PANC-1 cells revealed increased resistance in RES cells. (G) A Venn diagram comparing upregulated genes from RES PANC-1 cells, RES patient tissues, and GSE62452 tumor samples identified SLC5A3 among the commonly upregulated genes.

3.4. SLC5A3 depletion induces mitochondrial apoptosis and ROS

We performed transcriptomic analysis comparing SLC5A3 knockdown (KD) cells with control RES cells. Functional annotation via Gene Ontology (GO) revealed a strong enrichment of pathways related to apoptotic regulation and oxidative stress responses in KD cells (Figure 4A), suggesting that SLC5A3 supports cell survival under cytotoxic conditions. Consistently, Gene Set Enrichment Analysis (GSEA) identified upregulation of both programmed cell death and ROS-associated gene networks upon SLC5A3 suppression (Figure 4B).

To validate these findings experimentally, we employed Annexin V staining to quantify apoptotic activity. KD cells exhibited a significantly elevated percentage of Annexin V-positive populations relative to both sensitive (SEN) and RES control groups, supporting the notion that SLC5A3 loss induces cell death (Figure 4C). Since intrinsic apoptosis is often linked to mitochondrial perturbation, we assessed membrane potential using the JC-10 probe. KD cells displayed a notable reduction in mitochondrial potential, indicative of functional impairment of the organelle (Figure 4D). We next examined the expression levels of genes involved in apoptosis. Quantitative analysis showed that silencing SLC5A3 led to a decrease in anti-apoptotic BCL2 transcripts and an increase in pro-apoptotic genes such as BAX, CASP3, and CASP9 (Figure 4E). At the protein level, expression of cleaved CASP9, CASP8, BAX, PUMA, and PARP was elevated in KD cells, confirming the activation of intrinsic apoptotic signaling cascades (Figure 4F).

Given that GSEA results highlighted ROS pathway involvement (Figure 4B), we investigated intracellular ROS accumulation. Fluorescence-based assays revealed that ROS levels were significantly increased in KD cells compared to both SEN and RES controls (Figure 4G), aligning with previously established roles of ROS in mediating apoptotic cell fate. [37,38]

To determine whether antioxidant defenses were disrupted, we measured the expression of NRF2 and GPX4, two pivotal components of the cellular redox response. Both markers were significantly downregulated following SLC5A3 knockdown (Figure 4H), suggesting that oxidative imbalance was exacerbated by impaired antioxidant capacity.

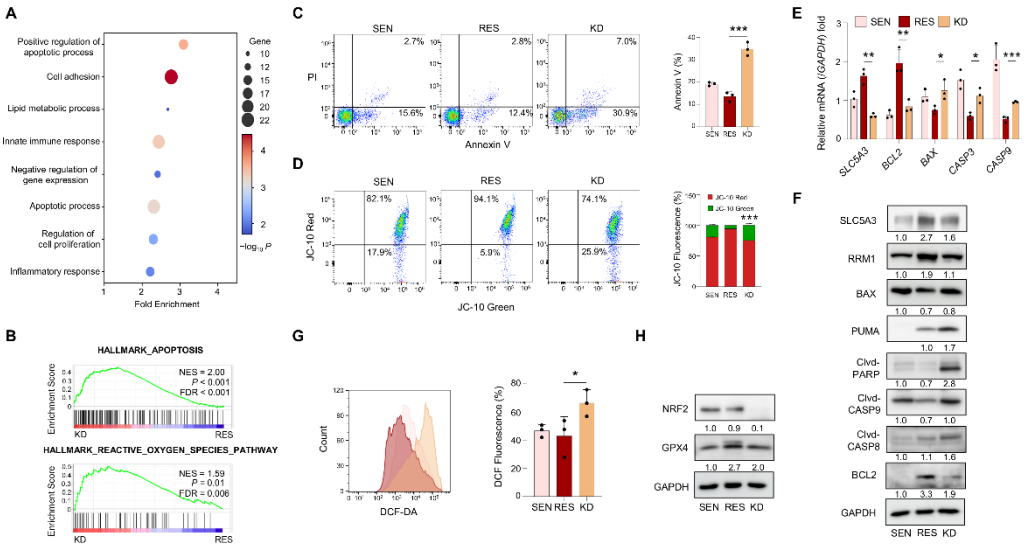

Figure 4. SLC5A3 depletion induces mitochondrial apoptosis and ROS. (A) GO analysis revealed enrichment of apoptosis and oxidative stress pathways following SLC5A3 knockdown. (B) GSEA showed significant upregulation of apoptotic and ROS-related gene sets in KD cells. (C) Annexin V staining demonstrated increased apoptotic cell populations in KD cells. (D) JC-10 staining showed reduced mitochondrial membrane potential in knockdown cells. (E) mRNA expression of BCL2 was decreased, while BAX, CASP3, and CASP9 were elevated. (F) Western blotting revealed increased levels of cleaved apoptotic proteins. (G) Intracellular ROS levels were significantly higher in KD cells. (H) NRF2 and GPX4 expression was diminished, suggesting impaired antioxidant defense mechanisms.

3.5. SLC5A3 depletion alters mitochondria and triggers mitophagic cell death

The regulation of mitochondrial dynamics is essential for preserving cellular equilibrium, and disturbances in this process can lead to mitochondrial dysfunction and cell demise. [39,40] Based on previous evidence suggesting a regulatory role for SLC5A3 in mitochondrial integrity [41,42], we investigated whether SLC5A3 knockdown (KD) alters mitochondrial behavior in gemcitabine-resistant PDAC cells. A heatmap comparison revealed that SLC5A3 knockdown led to a notable increase in pro-apoptotic gene expression and a concurrent reduction in anti-apoptotic gene levels (Figure 5A), suggesting that silencing SLC5A3 induces a gene expression profile characteristic of apoptosis.

To further examine mitochondrial alterations, we performed transmission electron microscopy (TEM). KD cells exhibited abnormal mitochondrial morphologies characterized by increased fragmentation, disrupted cristae, spherical shape, and vacuolization—features indicative of mitochondrial stress (Figure 5B). These results suggest enhanced mitochondrial fission in the absence of SLC5A3. [43] High-content image analysis supported these findings, showing that KD cells had a greater number of mitochondria with reduced average size (Figure 5C). [44] In addition, MitoTracker staining showed evidence of mitochondrial division and structural compromise following SLC5A3 depletion (Figure 5D).

We then measured protein expression of fusion and fission regulators. SLC5A3 KD led to a decrease in mitochondrial fusion proteins OPA1 and MFN1, and an increase in the fission protein FIS1, indicating disruption of mitochondrial dynamics (Figure 5E).

To assess mitochondrial functionality, we measured the oxygen consumption rate (OCR). SLC5A3-deficient cells showed significantly reduced OCR, suggesting impaired mitochondrial respiration (Figure 5F). Consistent with this, mitochondrial ATP decreased while glycolytic ATP output increased in knockdown cells, highlighting a transition in cellular metabolism from mitochondrial respiration to glycolytic energy production (Figure 5G). Such a metabolic transition is indicative of impaired mitochondria that fail to sustain adequate energy production. [45,46] Reduced extracellular acidification rates in KD cells further confirmed the compromise in mitochondrial energy output. After observing mitochondrial abnormalities, we investigated whether the loss of SLC5A3 induces mitophagy, the targeted clearance of mitochondria. LC3B and MitoTracker staining demonstrated enhanced mitophagy in cells lacking SLC5A3 (Figure 5H). Furthermore, immunoblot analysis of mitochondrial fractions confirmed elevated levels of mitophagy markers following SLC5A3 silencing (Figure 5I). Interestingly, despite mitophagy's normal function in maintaining cellular health by clearing damaged mitochondria [11,15], we observed a net decrease in total mitochondrial content in KD cells based on both MitoTracker signal and TEM observations. These data suggest that mitophagy became excessive, leading to the depletion of even healthy mitochondria. This process was likely exacerbated by the concurrent loss of fusion-related proteins and increase in fission regulators, further amplifying mitochondrial disintegration.

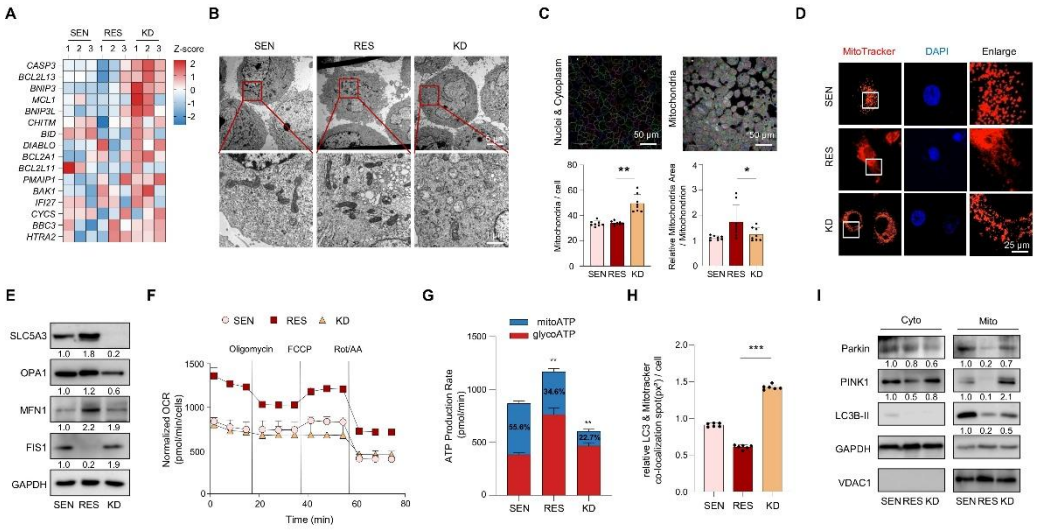

Figure 5. SLC5A3 depletion alters mitochondria and triggers mitophagic cell death. (A) Heatmap of gene expression showed that SLC5A3 knockdown increased pro-apoptotic and decreased anti-apoptotic gene expression. (B) TEM imaging revealed mitochondrial fragmentation and structural abnormalities in KD cells. (C) High-content image analysis quantified an increase in mitochondrial number and a reduction in size. (D) MitoTracker staining revealed increased mitochondrial fragmentation following SLC5A3 knockdown, indicating enhanced fission activity. (E) Western blot results showed decreased fusion proteins (OPA1, MFN1) and increased FIS1. (F) OCR analysis indicated suppressed mitochondrial respiration. (G) ATP assays showed a metabolic shift from mitochondrial to glycolytic ATP production. (H) Confocal microscopy showed increased colocalization of LC3B and MitoTracker, suggesting mitophagy. (I) Immunoblot of mitochondrial fractions confirmed higher expression of mitophagy-related proteins.

3.6. SLC5A3 depletion impairs tumor progression and mitochondrial integrity in vivo

To evaluate the physiological relevance of SLC5A3 in regulating tumor development and mitochondrial homeostasis in gemcitabine-resistant pancreatic ductal adenocarcinoma (PDAC), we utilized an orthotopic xenograft model in BALB/c nude mice. To establish the orthotopic tumor model, 2.5×10^6 PANC-1 SEN or RES cells were injected into the pancreas of each immunodeficient mouse, with five mice allocated to each group. Eight weeks after implantation, SLC5A3 was silenced in vivo using lentiviral delivery of shRNA constructs (shSLC5A3), while a scrambled shRNA sequence served as control. Mice were further treated with gemcitabine and carbonyl cyanide m-chlorophenyl hydrazone (CCCP), a well-characterized mitochondrial uncoupler, to examine the interplay between mitochondrial activity and tumor suppression (Figure 6A). [47]

Tumor burden was assessed post-treatment. Both SLC5A3 silencing and CCCP administration led to significant reductions in tumor volume and weight compared to the untreated RES control group, indicating impaired tumor progression upon mitochondrial disruption (Figure 6B, C). Gene and protein expression analyses from excised tumor tissues showed that the depletion of SLC5A3 resulted in decreased levels of key cell cycle regulators, including CDK4 and CCND1, while promoting the expression of apoptotic and mitochondrial markers such as BAX and CASP3 (Figure 6D, E). These molecular shifts suggested compromised proliferative signaling and enhanced cell death.

To further validate mitochondrial alterations in vivo, immunofluorescence analysis was performed. Tumors from SLC5A3-depleted and CCCP-treated groups exhibited decreased staining for mitochondrial quality control proteins PINK1 and PARKIN, as well as reduced anti-apoptotic BCL2 expression. In contrast, levels of cleaved CASP3 were significantly increased, reinforcing the conclusion that mitochondrial dysfunction and apoptosis were both activated in these tumors (Figure 6F).

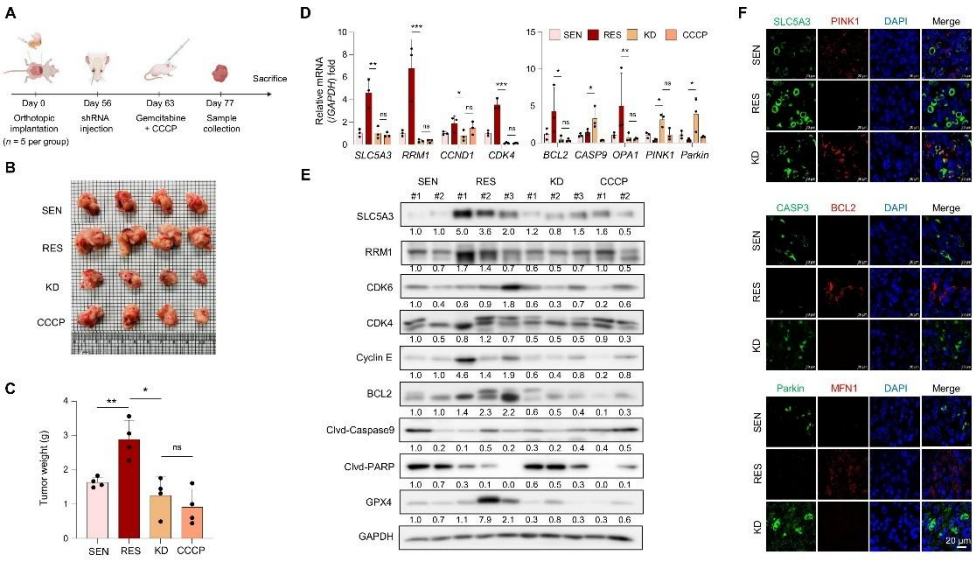

Figure 6. SLC5A3 depletion impairs tumor progression and mitochondrial integrity in vivo. (A) Experimental design: PANC-1 SEN and RES cells were orthotopically implanted into mice, followed by shRNA injection and treatment with gemcitabine and CCCP. (B, C) Tumor weight and volume were significantly lower in shSLC5A3- and CCCP-treated groups. (D, E) mRNA and protein analyses showed downregulation of CDK4 and CCND1 and upregulation of pro-apoptotic markers in treated tumors. (F) Immunofluorescence staining demonstrated decreased expression of PINK1, PARKIN, and BCL2, alongside an increase in cleaved CASP3 levels in both the SLC5A3 knockdown and CCCP-treated groups.

4. DISCUSSION

Gemcitabine resistance continues to pose a significant obstacle in the treatment of pancreatic ductal adenocarcinoma (PDAC), with prior studies implicating factors such as altered drug metabolism and enhanced pro-survival signaling pathways. [48,49,50] However, the complexity of chemoresistance suggests the involvement of additional cellular processes. This study revealed that SLC5A3 functions as a critical modulator contributing to gemcitabine resistance in PDAC, as demonstrated in Figures 1 and 2. SLC5A3 was found to be upregulated in resistant PDAC cells, and its inhibition led to impaired mitochondrial activity, elevated ROS levels, and induction of apoptosis, indicating its role in supporting cell survival under chemotherapy.

Though SLC5A3 is primarily known as a sodium/myo-inositol transporter [21], our findings expand its functional profile by demonstrating its involvement in mitochondrial regulation. Specifically, knockdown of SLC5A3 caused increased mitochondrial fragmentation, a decline in ATP synthesis, and elevated oxidative stress (Figure 5). Mitochondrial division, which often precedes mitophagy through the PINK1/Parkin signaling cascade [51,52,53], was notably accelerated. Interestingly, in SLC5A3-deficient cells, both damaged and functional mitochondria were removed, suggesting an overactivation of mitophagy that led to energetic collapse and apoptotic progression (Figure 4). This observation is consistent with reports linking mitochondrial instability to drug resistance in other cancer types such as breast and ovarian tumors [54,55], implying that targeting mitophagy may be beneficial in PDAC.

A significant association was also observed between SLC5A3 expression and oxidative phosphorylation (OXPHOS) capacity (Figure 5F). Chemoresistant tumors often enhance OXPHOS to fulfill elevated energy requirements. [56,57] In this study, the loss of SLC5A3 markedly diminished mitochondrial respiration and total ATP output, thereby disturbing cellular energy balance (Figure 5G). ATP depletion is known to impair essential cellular activities and amplify ROS accumulation by hindering oxidative repair mechanisms. [58,59,60] These changes promote a pro-apoptotic environment, as was evident in SLC5A3-deficient cells.

SLC5A3 inhibition also interfered with cell cycle progression (Figure 3). Depletion of SLC5A3 caused an accumulation of cells in the G1 phase and was associated with reduced expression of cyclin D1 and CDK4/6, aligning with earlier findings. [61,62] Mitochondrial health is sustained through a finely tuned balance between processes such as biogenesis, fusion, fission, and mitophagy. [63] Disruption of this balance by loss of mitochondrial content or function compromises overall cell viability. [64,65] Our data suggest that SLC5A3 contributes to this balance by maintaining mitochondrial structure and suppressing excessive mitophagy in chemoresistant cells. Future research should investigate how SLC5A3 interfaces with critical mitochondrial regulatory proteins such as DRP1, MFN2, and OPA1, which may uncover deeper insights into its involvement in energy homeostasis and structural integrity in cancer cells.

5. CONCLUSION

This study identifies SLC5A3 as a critical regulator of mitochondrial dynamics, cell cycle progression, and chemoresistance in pancreatic ductal adenocarcinoma (PDAC). SLC5A3 promotes gemcitabine resistance by preserving mitochondrial integrity, modulating cell cycle checkpoints, and limiting ROS-induced apoptosis. Conversely, SLC5A3 inhibition disrupts these pathways, resulting in enhanced apoptosis and increased sensitivity to chemotherapy. These findings position SLC5A3 as a potential therapeutic target for overcoming gemcitabine resistance in PDAC, particularly in treatment-refractory cases.

REFERENCES

1. Siegel RL, Giaquinto AN, Jemal A. Cancer statistics, 2024. CA Cancer J Clin. 2024;74:12–49.
2. Mizrahi JD, Surana R, Valle JW, Shroff RT. Pancreatic cancer. Lancet. 2020;395:2008–20.
3. Koltai T, Reshkin SJ, Carvalho TMA, Di Molfetta D, Greco MR, Alfarouk KO, et al. Resistance to gemcitabine in pancreatic ductal adenocarcinoma: a physiopathologic and pharmacologic review. Cancers (Basel). 2022;14:2486.
4. Qin C, Yang G, Yang J, Ren B, Wang H, Chen G, et al. Metabolism of pancreatic cancer: paving the way to better anticancer strategies. Mol Cancer. 2020;19:50.
5. Yang G, Guan W, Cao Z, Guo W, Xiong G, Zhao F, et al. Integrative genomic analysis of gemcitabine resistance in pancreatic cancer by patient-derived xenograft models. Clin Cancer Res. 2021;27:3383–96.
6. Gao HF, Chen LY, Cheng CS, Chen H, Meng ZQ, Chen Z. SLC5A1 promotes growth and proliferation of pancreatic carcinoma via glucose-dependent AMPK/mTOR signaling. Cancer Manag Res. 2019;11:3171–85.
7. Low HB, Wong ZL, Wu B, Kong LR, Png CW, Cho YL, et al. DUSP16 promotes cancer chemoresistance through regulation of mitochondria-mediated cell death. Nat Commun. 2021;12:2284.
8. Guo X, Yang N, Ji W, Zhang H, Dong X, Zhou Z, et al. Mito-Bomb: targeting mitochondria for cancer therapy. Adv Mater. 2021;33:e2007778.
9. Vyas S, Zaganjor E, Haigis MC. Mitochondria and cancer. Cell. 2016;166:555–66.
10. Boulton DP, Caino MC. Mitochondrial fission and fusion in tumor progression to metastasis. Front Cell Dev Biol. 2022;10:849962.
11. Willems PH, Rossignol R, Dieteren CE, Murphy MP, Koopman WJ. Redox homeostasis and mitochondrial dynamics. Cell Metab. 2015;22:207–18.
12. Li Y, Chen H, Xie X, Yang B, Wang X, Zhang J, et al. PINK1-mediated mitophagy promotes oxidative phosphorylation and redox homeostasis to induce drug-tolerant persister cancer cells. Cancer Res. 2023;83:398–413.
13. Chen W, Zhao H, Li Y. Mitochondrial dynamics in health and disease: mechanisms and potential targets. Signal Transduct Target Ther. 2023;8:333.
14. Guan Y, Wang Y, Li B, Shen K, Li Q, Ni Y, et al. Mitophagy in carcinogenesis, drug resistance and anticancer therapeutics. Cancer Cell Int. 2021;21:350.
15. Chen Y, Jiao D, Liu Y, Xu X, Wang Y, Luo X, et al. FBXL4 mutations cause excessive mitophagy via BNIP3/BNIP3L accumulation leading to mitochondrial DNA depletion syndrome. Cell Death Differ. 2023;30:2351–63.
16. Yang M, Wei X, Yi X, Jiang DS. Mitophagy-related regulated cell death: molecular mechanisms and disease implications. Cell Death Dis. 2024;15:505.
17. César-Razquin A, Snijder B, Frappier-Brinton T, Isserlin R, Gyimesi G, Bai X, et al. A call for systematic research on solute carriers. Cell. 2015;162:478–87.
18. Schlessinger A, Zatorski N, Hutchinson K, Colas C. Targeting SLC transporters: small molecules

as modulators and therapeutic opportunities. Trends Biochem Sci. 2023;48:801–14.
19. Puris E, Fricker G, Gynther M. The role of solute carrier transporters in efficient anticancer drug delivery and therapy. Pharmaceutics. 2023;15:364.
20. Wu Z, Xu J, Liang C, Meng Q, Hua J, Wang W, et al. Emerging roles of the solute carrier family in pancreatic cancer. Clin Transl Med. 2021;11:e356.
21. Dai G, Yu H, Kruse M, Traynor-Kaplan A, Hille B. Osmoregulatory inositol transporter SMIT1 modulates electrical activity by adjusting PI(4,5)P2 levels. Proc Natl Acad Sci USA. 2016;113:E3290–99.
22. Wei Y, Huang YH, Skopelitis DS, Iyer SV, Costa ASH, Yang Z, et al. SLC5A3-dependent myo-inositol auxotrophy in acute myeloid leukemia. Cancer Discov. 2022;12:450–67.
23. Cui Z, Mu C, Wu Z, Pan S, Cheng Z, Zhang ZQ, et al. The sodium/myo-inositol co-transporter SLC5A3 promotes non-small cell lung cancer cell growth. Cell Death Dis. 2022;13:569.
24. Li L, Shen FR, Cheng Q, Sun J, Li H, Sun HT, et al. SLC5A3 is important for cervical cancer cell growth. Int J Biol Sci. 2023;19:2787–802.
25. Kim MJ, Kim HS, Kang HW, Lee DE, Hong WC, Kim JH, et al. SLC38A5 modulates ferroptosis to overcome gemcitabine resistance in pancreatic cancer. Cells. 2023;12:2509.
26. Lee DE, Kang HW, Kim SY, Kim MJ, Jeong JW, Hong WC, et al. Ivermectin and gemcitabine combination treatment induces apoptosis of pancreatic cancer cells via mitochondrial dysfunction. Front Pharmacol. 2022;13:934746.
27. Tang Z, Li C, Kang B, Gao G, Li C, Zhang Z. GEPIA: a web server for cancer and normal gene expression profiling and interactive analyses. Nucleic Acids Res. 2017;45:W98–102.
28. Uhlen M, Zhang C, Lee S, Sjöstedt E, Fagerberg L, Bidkhori G, et al. A pathology atlas of the human cancer transcriptome. Science. 2017;357:6352.
29. Weinstein JN, Collisson EA, Mills GB, Shaw KR, Ozenberger BA, Ellrott K, et al. The cancer genome atlas pan-cancer analysis project. Nat Genet. 2013;45:1113–20.
30. Lonsdale J, Thomas J, Salvatore M, Phillips R, Lo E, Shad S, et al. The genotype-tissue expression (GTEx) project. Nat Genet. 2013;45:580–5.
31. Liu J, Lichtenberg T, Hoadley KA, Poisson LM, Lazar AJ, Cherniack AD, et al. An integrated TCGA pan-cancer clinical data resource to drive high-quality survival outcome analytics. Cell. 2018;173:400–16.e11.
32. Ashburner M, Ball CA, Blake JA, Botstein D, Butler H, Cherry JM, et al. Gene ontology: tool for the unification of biology. The Gene Ontology Consortium. Nat Genet. 2000;25:25–29.
33. Jordheim LP, Sève P, Trédan O, Dumontet C. The ribonucleotide reductase large subunit (RRM1) as a predictive factor in patients with cancer. Lancet Oncol. 2011;12:693–702.
34. Berry GT, Mallee JJ, Kwon HM, Rim JS, Mulla WR, Muenke M, et al. The human osmoregulatory Na+/myo-inositol cotransporter gene (SLC5A3): molecular cloning and localization to chromosome 21. Genomics. 1995;25:507–13.
35. Bizzarri M, Dinicola S, Bevilacqua A, Cucina A. Broad spectrum anticancer activity of myo-inositol and inositol hexakisphosphate. Int J Endocrinol. 2016;2016:5616807.
36. Subramanian A, Tamayo P, Mootha VK, Mukherjee S, Ebert BL, Gillette MA, et al. Gene set enrichment analysis: a knowledge-based approach for interpreting genome-wide expression profiles.

Proc Natl Acad Sci USA. 2005;102:15545–50.
37. Böhme R, Schmidt AW, Hesselbarth N, Posern G, Sinz A, Ihling C, et al. Induction of oxidative- and endoplasmic-reticulum-stress dependent apoptosis in pancreatic cancer cell lines by DDOST knockdown. Sci Rep. 2024;14:20388.
38. Tan SN, Sim SP, Khoo AS. Potential role of oxidative stress-induced apoptosis in mediating chromosomal rearrangements in nasopharyngeal carcinoma. Cell Biosci. 2016;6:35.
39. Anderson GR, Wardell SE, Cakir M, Yip C, Ahn YR, Ali M, et al. Dysregulation of mitochondrial dynamics proteins are a targetable feature of human tumors. Nat Commun. 2018;9:1677.
40. Courtois S, de Luxán-Delgado B, Penin-Peyta L, Royo-García A, Parejo-Alonso B, Jagust P, et al. Inhibition of mitochondrial dynamics preferentially targets pancreatic cancer cells with enhanced tumorigenic and invasive potential. Cancers (Basel). 2021;13:698.
41. Toker L, Bersudsky Y, Plaschkes I, Chalifa-Caspi V, Berry GT, Buccafusca R, et al. Inositol-related gene knockouts mimic lithium's effect on mitochondrial function. Neuropsychopharmacology. 2014;39:319–28.
42. Hsu CC, Zhang X, Wang G, Zhang W, Cai Z, Pan BS, et al. Inositol serves as a natural inhibitor of mitochondrial fission by directly targeting AMPK. Mol Cell. 2021;81:3803–19.e7.
43. Toyama EQ, Herzig S, Courchet J, Lewis TL Jr., Losón OC, Hellberg K, et al. Metabolism. AMP-activated protein kinase mediates mitochondrial fission in response to energy stress. Science. 2016;351:275–81.
44. Rees DJ, Roberts L, Carla Carisi M, Morgan AH, Brown MR, Davies JS. Automated quantification of mitochondrial fragmentation in an in vitro parkinson's disease model. Curr Protoc Neurosci. 2020;94:e105.
45. Giddings EL, Champagne DP, Wu MH, Laffin JM, Thornton TM, Valenca-Pereira F, et al. Mitochondrial ATP fuels ABC transporter-mediated drug efflux in cancer chemoresistance. Nat Commun. 2021;12:2804.
46. Al Assi A, Posty S, Lamarche F, Chebel A, Guitton J, Cottet-Rousselle C, et al. A novel inhibitor of the mitochondrial respiratory complex I with uncoupling properties exerts potent antitumor activity. Cell Death Dis. 2024;15:311.
47. Koncha RR, Ramachandran G, Sepuri NBV, Ramaiah KVA. CCCP-induced mitochondrial dysfunction - characterization and analysis of integrated stress response to cellular signaling and homeostasis. Febs J. 2021;288:5737–54.
48. Chen C, Zhao S, Zhao X, Cao L, Karnad A, Kumar AP, et al. Gemcitabine resistance of pancreatic cancer cells is mediated by IGF1R dependent upregulation of CD44 expression and isoform switching. Cell Death Dis. 2022;13:682.
49. Li W, Zhu Y, Zhang K, Yu X, Lin H, Wu W, et al. PROM2 promotes gemcitabine chemoresistance via activating the Akt signaling pathway in pancreatic cancer. Exp Mol Med. 2020;52:409–22.
50. Cao L, Huang C, Cui Zhou D, Hu Y, Lih TM, Savage SR, et al. Proteogenomic characterization of pancreatic ductal adenocarcinoma. Cell. 2021;184:5031–52.e26.
51. Li Q, Chu Y, Li S, Yu L, Deng H, Liao C, et al. The oncoprotein MUC1 facilitates breast cancer progression by promoting Pink1-dependent mitophagy via ATAD3A destabilization. Cell Death Dis.

2022;13:899.
52. Yao N, Wang C, Hu N, Li Y, Liu M, Lei Y, et al. Inhibition of PINK1/Parkin-dependent mitophagy sensitizes multidrug-resistant cancer cells to B5G1, a new betulinic acid analog. Cell Death Dis. 2019;10:232.
53. Qin C, Wang Y, Zhao B, Li Z, Li T, Yang X, et al. STOML2 restricts mitophagy and increases chemosensitivity in pancreatic cancer through stabilizing PARL-induced PINK1 degradation. Cell Death Dis. 2023;14:191.
54. Meng Y, Qiu L, Zeng X, Hu X, Zhang Y, Wan X, et al. Targeting CRL4 suppresses chemoresistant ovarian cancer growth by inducing mitophagy. Signal Transduct Target Ther. 2022;7:388.
55. Zhen Y, Yuan Z, Zhang J, Chen Y, Fu Y, Liu Y, et al. Flubendazole induces mitochondrial dysfunction and DRP1-mediated mitophagy by targeting EVA1A in breast cancer. Cell Death Dis. 2022;13:375.
56. Boykov IN, Montgomery MM, Hagen JT, Aruleba RT, McLaughlin KL, Coalson HS, et al. Pan-tissue mitochondrial phenotyping reveals lower OXPHOS expression and function across cancer types. Sci Rep. 2023;13. 16742.
57. Masoud R, Reyes-Castellanos G, Lac S, Garcia J, Dou S, Shintu L, et al. Targeting mitochondrial complex I overcomes chemoresistance in high OXPHOS pancreatic cancer. Cell Rep. Med. 2020;1:100143.
58. Imamura H, Sakamoto S, Yoshida T, Matsui Y, Penuela S, Laird DW, et al. Single-cell dynamics of pannexin-1-facilitated programmed ATP loss during apoptosis. Elife. 2020;9:e61960.
59. Ebanks B, Chakrabarti L. Mitochondrial ATP synthase is a target of oxidative stress in neurodegenerative diseases. Front Mol Biosci. 2022;9:854321.
60. Wang SF, Tseng LM, Lee HC. Role of mitochondrial alterations in human cancer progression and cancer immunity. J Biomed Sci. 2023;30:61.
61. Salvador-Barbero B, Álvarez-Fernández M, Zapatero-Solana E, El Bakkali A, Menéndez MDC, López-Casas PP, et al. CDK4/6 inhibitors impair recovery from cytotoxic chemotherapy in pancreatic adenocarcinoma. Cancer Cell. 2020;37:340–53.e6.
62. Pandini C, Pagani G, Tassinari M, Vitale E, Bezzecchi E, Saadeldin MK, et al. The pancancer overexpressed NFYC Antisense 1 controls cell cycle mitotic progression through in cis and in trans modes of action. Cell Death Dis. 2024;15:206.
63. Masuo H, Kubota K, Shimizu A, Notake T, Miyazaki S, Yoshizawa T, et al. Increased mitochondria are responsible for the acquisition of gemcitabine resistance in pancreatic cancer cell lines. Cancer Sci. 2023;114:4388–4400.
64. Zong Y, Li H, Liao P, Chen L, Pan Y, Zheng Y, et al. Mitochondrial dysfunction: mechanisms and advances in therapy. Signal Transduct Target Ther. 2024;9:124.
65. Ma K, Chen G, Li W, Kepp O, Zhu Y, Chen Q. Mitophagy, mitochondrial homeostasis, and cell fate. Front Cell Dev Biol. 2020;8:467.

Abstract in Korean

췌장암의 젬시타빈 저항성 억제 신규 유전자 발굴

췌장암은 치료에 대한 내성이 빠르게 발생하여 예후가 불량한 악성 종양이다. 미토콘드리아 역학은 암세포 생존에 중요한 역할을 하지만, 췌장암에서 젬시타빈 저항성을 유도하는 구체적인 기전은 아직 명확히 규명되지 않았다.

본 연구에서는 나트륨/미오이노시톨 공동수송체인 SLC5A3 이 췌장암에서 젬시타빈 저항성을 촉진하는 주요 조절인자임을 규명했다. 젬시타빈 저항성을 갖는 췌장암 세포에서 SLC5A3의 발현이 유의미하게 증가하였으며, SLC5A3의 억제는 세포 생존력을 현저히 감소시켰다. 미토콘드리아 분석 결과, SLC5A3 억제가 미토콘드리아 역학을 교란시키며, 이로 인해 활성산소 생성 증가, 미토콘드리아 분열 촉진, 그리고 산화적 인산화 기능 저하를 유도함을 확인했다.

또한, SLC5A3 억제가 PINK1/Parkin 매개 mitophagy를 활성화하여, 손상된 미토콘드리아뿐만 아니라 정상적인 미토콘드리아까지 과도하게 제거함을 입증했다. 이러한 미토콘드리아 감소는 세포를 apoptosis에 더욱 취약하게 만드는 것으로 나타났다. In vivo 연구에서도 SLC5A3을 표적화하면 젬시타빈 치료 효과가 증대되며, 종양 성장 또한 유의미하게 감소하는 것을 확인했다.

이러한 연구 결과는 SLC5A3이 미토콘드리아 조절을 통해 췌장암의 젬시타빈 저항성에서 중요한 역할을 하며, 나아가 SLC5A3이 젬시타빈 저항성을 극복하기 위한 유망한 치료 표적이 될 가능성을 시사한다.

핵심되는 말: 췌장암, 젬시타빈, 항암제 저항성, 미토콘드리아 기능장애, 미토파지